Analysis of the effect of flow-induced crystallization on the stability of low-speed spinning using the linear stability method

Dong Myeong Shin, Joo Sung Lee, Hyun Wook Jung* and Jae Chun Hyun
*Department of Chemical and Biological Engineering, Applied Rheology Center,
Korea University, Seoul 136-701, Korea*

(Received May 2, 2005)

Abstract

The stability of low-speed spinning process exhibiting spinline flow-induced crystallization (FIC) with no neck-like spinline deformation has been investigated using the method of linear stability analysis. Effects of various process conditions such as fluid viscoelasticity and the spinline cooling on the spinning stability have been found closely related to the development of the spinline crystallinity. It also has been found that the FIC makes the system less stable or more unstable than no FIC cases when the spinline crystallinity reaches its maximum possible value, whereas the FIC generally stabilizes the system if the crystallinity doesn't reach its maximum value on the spinline. It is believed that the destabilizing effect of the FIC on low-speed spinning when the crystallinity is fully developed on the spinline is due to the reduction of the real spinning length available for deformation on the spinline. On the other hand, the increased spinline tension caused by the FIC when the maximum crystallinity is not reached on the spinline and thus no reduction in the spinning length occurs, makes the sensitivity of spinline variables to external disturbances smaller and hence stabilizes the system. These linear stability results are consistent with the findings by nonlinear transient simulation, as first reported by Lee *et al.* (2005b).

Keywords : draw resonance, fiber spinning, flow-induced crystallization, linear stability analysis, crystallinity, stability windows

1. Introduction

The fundamental aspects of draw resonance instability occurring in the polymer extensional deformation processes such as fiber spinning, film casting, and tubular film blowing have been steadily elucidated by many researchers during the last four decades (Gelder, 1971; Fisher and Denn, 1976; Hyun, 1978; Schultz *et al.*, 1984; Liu and Beris, 1988; Jung *et al.*, 2000; Hatzikiriakos and Migler, 2005; Lee *et al.*, 2005a) ever since it was first experimentally observed and named as such in the early 1960s (Christensen, 1962; Miller, 1963). This instability, well known as a supercritical Hopf bifurcation, is characterized by the sustained periodic oscillation of spinline dependent variables like cross-sectional area and tension (Schultz *et al.*, 1984). The study on draw resonance is quite important industrially as well as academically because it is closely related to productivity, high quality control of products and also its theoretical analysis involves the fundamental understanding of the nonlinear dynamics of the processes.

Despite great scientific progress in the stability and sen-

sitivity problems of spinning processes, especially in draw resonance instability, there are some unsettled issues as expounded by Petrie (1988). One salient example is the nonlinear dynamics and stability of the low or high-speed spinning when the flow-induced crystallization (FIC) occurs on the spinline. Recently, Lee *et al.* (2005b) for the first time solved the transient responses of low-speed spinning accompanied by this FIC by developing a robust numerical algorithm able to handle high stress level at the spinneret. They reported that the FIC destabilizes the spinning system as compared to the case with no crystallization when the spinline crystallinity reaches its maximum possible value on the spinline.

In this sequel to Lee *et al.* (2005b) the study of the stability of low-speed spinning with the flow-induced crystallization has been extended using a typical stability tool, i.e., linear stability analysis, to examine the effect of various process conditions on the process stability.

2. Governing equations for spinning flows

The same non-dimensionalized governing equations for viscoelastic spinning system with flow-induced crystallization kinetics as developed by Lee *et al.* (2005b), where
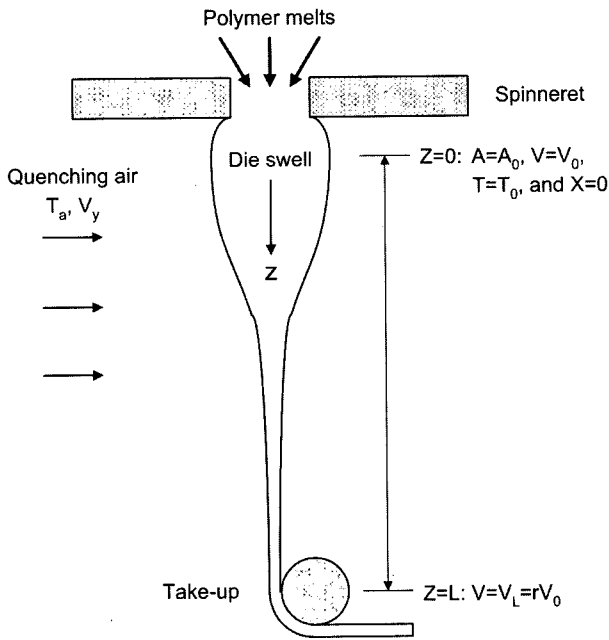
Fig. 1. Schematic diagram of fiber spinning process.

no neck-like deformation occurs on the spinline, have been used in this study (Fig. 1 shows the schematic of this spinning process.). Phan-Thien and Tanner (PTT) equation as a viscoelastic constitutive model, well known for its robustness and accuracy in describing extensional deformation processes, was employed (Phan-Thien, 1978). To simulate the spinning process with crystallization a one-phase crystallization model was adopted in the governing equations, as similarly employed by Joo et al. (2002) and Patel et al. (1991). (Although the two-phase model developed by Doufas et al. (2000a; 2000b) treating the crystalline and amorphous phases within the spinline separately possesses more flexibilities for portraying the morphological characteristics of the spinline, the one-phase model has been lately found equally capable in portraying the same spinline characteristic, e.g., neck-like deformation in high-speed spinning, with a much smaller number of parameters required for the model (Shin et al., 2005).)

Also it has already been confirmed (Lee et al., 2005b) that this model well predicts quantitatively the experimental steady profiles by Kolb et al. (2000).

Equation of continuity:

$$\frac{\partial a}{\partial t} + \frac{\partial (av)}{\partial z} = 0, \tag{1}$$

where, $a = \dfrac{A}{A_0}$, $v = \dfrac{V}{V_0}$, $t = \dfrac{t^* V_0}{L}$, $z = \dfrac{Z}{L}$.

Equation of motion:

$$C_{in}\left(\frac{\partial v}{\partial t} + v\frac{\partial v}{\partial z}\right) = \frac{1}{a}\frac{\partial (a\tau)}{\partial z} + C_{gr} - C_{ad}v^{1.19}a^{-0.905}, \tag{2}$$

where, $C_{in} = \dfrac{\rho V_0 L}{2\eta_0}$, $C_{gr} = \dfrac{\rho g L^2}{2\eta_0 V_0}$, $C_{ad} = \dfrac{3.122 \times 10^{-4} V_0^{1.19} L^2}{2A_0^{0.905}\eta_0}$,

$$\tau = \frac{\sigma}{2\eta_0 V_0 / L}.$$

Constitutive equation (PTT fluids):

$$K\tau + De\left[\frac{\partial \tau}{\partial t} + v\frac{\partial \tau}{\partial z} - 2(1-\xi)\tau\frac{\partial v}{\partial z}\right] = \frac{\eta}{\eta_0}\frac{\partial v}{\partial z}, \tag{3}$$

where, $K = \exp\left[\dfrac{2\varepsilon De_0 \tau}{\exp(3.2x)}\right]$, $De = \dfrac{\lambda V_0}{L}$, $De_0 = \dfrac{\lambda_0 V_0}{L}$,

$$De = De_0\exp\left[\frac{E}{RT_0}\left(\frac{1}{\theta}-1\right)+(\alpha^*-3.2)x\right],$$

$$\eta = \eta_0\exp\left[\frac{E}{RT_0}\left(\frac{1}{\theta}-1\right)+\alpha^*x\right].$$

Equation of energy:

$$\frac{\partial \theta}{\partial t} + v\frac{\partial \theta}{\partial z} = -Stv^{1/3}a^{-5/6}(\theta-\theta_a)\left[1+64\left(\frac{v_y}{v}\right)^2\right]^{1/6} + \Delta H_f\left(\frac{\partial x}{\partial t}+v\frac{\partial x}{\partial z}\right), \tag{4}$$

where, $St = \dfrac{1.67\times 10^{-4}L}{\rho C_p V_0^{1/3}A_0^{5/6}}$, $\theta = \dfrac{T}{T_0}$, $\theta_a = \dfrac{T_a}{T_0}$, $v_y = \dfrac{V_y}{V_0}$,

$$\Delta H_f = \frac{\Delta H_f^* X_\infty}{C_p T_0}.$$

Crystallinity equation:

$$\frac{\partial x}{\partial t} + v\frac{\partial x}{\partial z} = n\left[\ln\left(\frac{1}{1-x}\right)\right]^{(n-1)/n}(1-x)k_m$$

$$\times\exp\left[-4\ln 2\left(\frac{\theta-\theta_{max}}{d}\right)^2 + 2\kappa\tau De_0\right], \tag{5}$$

where, $x = \dfrac{X}{X_\infty}$, $k_m = \dfrac{K_{max}L}{V_0}$, $\theta_{max} = \dfrac{T_{max}}{T_0}$, $d = \dfrac{D}{T_0}$.

Boundary conditions:

$$a_0 = 1, \ v_0 = 1, \ \theta_0 = 1, \ x_0 = 0 \ \text{at } z = 0 \ \text{for all } t \tag{6a}$$

$$v_L = r \qquad\qquad \text{at } z = 1 \ \text{for all } t \tag{6b}$$

where a, v, t, z, and Ω denote the dimensionless spinline cross-sectional area, spinline velocity, time, distance in the flow direction, and fluid axial extra stress, respectively, C_{in} the inertia coefficient, C_{gr} the gravity coefficient, C_{ad} the air-drag coefficient, ρ the fluid density, L the spinning distance, g the gravity acceleration constant, De the Deborah number, λ the fluid relaxation time, ε and ξ the PTT model parameters, η the fluid shear viscosity, α^* the model parameter representing the crystallinity dependency of the viscosity, St the Stanton number, C_p the fluid heat capacity, n the Avrami index (unity value in this study), κ the flow-induced crystallization (FIC) enhancement factor representing the stress dependency of the crystallization rate following the similar models in the literature (Doufas et al., 2000a; Doufas et al., 2000b), r the draw ratio, and θ, θ_a,

ΔH_f, v_y, x, k_m, θ_{max}, and d the dimensionless spinline temperature, cooling air temperature, crystallization heat, cooling air velocity, spinline crystallinity, maximum crystallization rate, temperature at maximum crystallization rate, and crystallization half width temperature range, respectively. Subscripts 0 and L mean die exit and take-up conditions, respectively.

The fluid viscosity and the relaxation time are the functions of both temperature and crystallinity preventing an abnormal increase in the spinline stress, whereas the fluid modulus is mainly dependent on the crystallinity (Muslet and Kamal, 2004). It is noted that the trace of extra stress tensor in the flow-induced term in the crystallinity equation is simply reduced to the single axial extra stress, τ, in our 1-D model.

3. Linear stability analysis

The first step for the linear stability analysis is to linearize the above governing equations, Eqs. (1)-(5), by introducing the infinitesimal perturbations to state variables around their steady states as follows.

$$a(t, z) = a_s(z) + \alpha(z)\exp(\Omega t), \quad v(t, z) = v_s(z) + \beta(z)\exp(\Omega t),$$
$$\tau(t, z) = \tau_s(z) + \gamma(z)\exp(\Omega t), \quad \theta(t, z) = \theta_s(z) + \delta(z)\exp(\Omega t),$$
$$x(t, z) = x_s(z) + \phi(z)\exp(\Omega t) \tag{7}$$

where subscript s indicates the steady state, Ω is a complex eigenvalue that accounts for the growth rate of the perturbation and α, β, γ, δ, and ϕ the perturbed quantities of state variables. Substitution of Eq. (7) into the governing equations leads to the following linearized governing equations.

Linearized equation of continuity:

$$\Omega\alpha = (v'_s)\alpha - (v'_s)\alpha' + \left(\frac{v'_s}{v_s^2}\right)\beta - \left(\frac{1}{v_s}\right)\beta' \tag{8}$$

Linearized equation of motion:

$$C_{in}\Omega\beta = (\tau_s v'_s + 0.905 C_{ad}v_s^{3.095})\alpha + (\tau_s v_s)\alpha'$$
$$-(C_{in}v'_s + 1.19 C_{ad}v_s^{1.095})\beta - (C_{in}v_s)\beta' - \left(\frac{v'_s}{v_s}\right)\gamma + \gamma' \tag{9}$$

Linearized constitutive equation (PTT fluids):

$$-\Omega\gamma = \left(\frac{2\varepsilon\tau_s E_1}{E_3\exp(3.2x_s)} + \frac{E_1}{De_0 E_3} - 2(1-\xi)v'_s\right)\gamma + (v_s)\gamma' + (\tau'_s)\beta$$

$$-\left(2(1-\xi)\tau_s + \frac{E_2}{De_0 E_3}\right)\beta$$

$$+\left(2(1-\xi)\tau_s v'_s \frac{E/RT_0}{\theta_s^2} + E_2 v'_s \frac{E/RT_0}{De_0 E_3 \theta_s^2} - \tau'_s v_s \frac{E/RT_0}{\theta_s^2}\right)\delta$$

$$+\left(\begin{array}{c} -6.4\frac{E_1}{E_3}\varepsilon\tau_s^2\exp(-3.2x_s) + (\alpha^* - 3.2)\tau'_s v_s \\ -2(1-\xi)(\alpha^* - 3.2)\tau_s v'_s - \frac{E_2}{De_0 E_3}\alpha^* v'_s \end{array}\right)\phi \tag{10}$$

where $E_1 = \exp\left[\frac{2\varepsilon De_0 \tau_s}{\exp(3.2x_s)}\right]$, $E_2 = \exp\left[\frac{E}{RT_0}\left(\frac{1}{\theta_s} - 1\right) + \alpha^* x_s\right]$,

$$E_3 = \exp\left[\frac{E}{RT_0}\left(\frac{1}{\theta_s} - 1\right) + (\alpha^* - 3.2)x_s\right]$$

Linearized equation of energy:

$$\Omega\delta - \Delta H_f\Omega\phi = \left(\frac{5}{6}Stv_s^{13/6}\Psi^{1/6}(\theta_s - \theta_a)\right)\alpha - (Stv_s^{7/6}\Psi^{1/6})\delta - (v_s)\delta'$$

$$+\left(-\theta'_s + \Delta H_f x'_s - \frac{1}{3}Stv_s^{1/6}\Psi^{1/6}(\theta_s - \theta_a)\right)$$

$$+\frac{64}{3}Stv_y^2 v_s^{-11/6}\Psi^{-5/6}(\theta_s - \theta_a)\right)\beta + (\Delta H_f v_s)\phi' \tag{11}$$

where $\Psi = \left(1 + 64\left(\frac{v_y}{v_s}\right)^2\right)$

Linearized crystallinity equation:

$$\Omega\phi = (-x'_s)\beta - \left(8(\ln 2)E_4(1-x_s)\frac{\theta_s - \theta_m}{d^2}\right)\delta - (E_4)\phi - (v_s)\phi'$$

$$+(2E_4(1-x_s)\kappa De_0)\gamma \tag{12}$$

where $E_4 = k_m\exp\left[-4\ln 2 F^2\left(\frac{\theta_s - \theta_m}{d}\right)^2 + 2\kappa\tau_s De_0\right]$

Boundary conditions:

$$\alpha(0) = \beta(0) = \beta(1) = \delta(0) = \phi(0) = 0 \tag{13}$$

In the above equations, superscript ' denotes derivative of state variables with respect to spinline distance, z. There are a couple of methods to evaluate eigenmodes using the above linearized equations. The first is to construct eigenmatrix system by discretizing the above linearized equations, Eqs. (8)-(13), using a proper finite difference scheme and rearranging them as follows (Gelder, 1971).

$$\Omega y = Jy \tag{14}$$

where $y = [\alpha, \beta, \gamma, \delta, \phi]$ and J is matrix whose components are obtained from the algebraic manipulations of Eqs. (8)-(13). The stability of the system is then determined by eigenvalues, Ω. If the real part of the leading eigenmode of Ω for a given condition is found positive, then the system is unstable indicating the unbounded growth of state variables with time.

The second involves an assumed scalar value for Ω and the 4th-order Runge-Kutta method with a shooting scheme, only focusing on the leading eigenvalue instead of its entire eigen-spectrum, resulting in the same stability data (Fisher and Denn, 1976). In this study, the latter has been adopted, giving the fast computation to obtain the leading eigenmode, compared to the former case.

4. Results and discussion

As an example fluid for analyzing the low-speed spinning stability with the FIC, isotactic polypropylene (iPP), known as a well-crystallizable polymer in the literature

Table 1. Model parameters for iPP.

Parameters	Values
Density, ρ (kg/m^3)	970
Heat capacity, C$_p$ (cal/g°C)	0.46
Zero-shear viscosity, η_0 (Poise)	34200
Relaxation time, λ_0 (s)	0.04
PTT model parameters, ε & ξ	0.015, 0.6
Dimensionless activation energy, E/R (K)	5.602 × 10^3
Heat of crystallization, ΔH_f (J/g)	148.453
Maximum crystallization rate, K_{max} (s^{-1})	0.55
Temperature at max. crystallization rate, T_{max} (K)	338
Crystallization half width temperature range, D (K)	333
Maximum crystallinity, X_∞ (%)	55
Crystallinity dependency parameter of viscosity, α	5.1
Flow-induced crystallization enhancement factor, κ	8.2

(Kolb et al., 2000) has been chosen. Some of the rheological properties and model parameters characterizing iPP including its extension thinning behavior, are summarized in Table 1 (Ziabicki, 1976; Minoshima et al., 1980; Kolb et al., 2000; Muslet and Kamal, 2004; Zheng and Kennedy, 2004).

As mentioned in Introduction, Lee et al. (2005b) first investigated the nonlinear dynamics and stability of this iPP spinning solving the same 1-D governing equations as in here to obtain the transient responses of the system for the first time. It was concluded there that the flow-induced crystallization makes the system less stable or more unstable than the case without crystallization, when the spinline crystallinity is fully developed to its maximum value. It is believed that the reason for the destabilizing effect of the FIC in the case with fully developed crystallinity is that maximum crystallinity shortens the real spinning length available for deformation on the spinline, and this shortened spinning length then destabilizes the spinning because increasing spinning length with other things kept constant is known to stabilize the system (Matsumoto and Bogue, 1978). In this paper, using the convenient linear stability method the effect of flow-induced crystallization kinetics on the process stability under various process conditions has been extensively analyzed.

Utilizing this stability method, it is possible to systematically construct the various stability windows for iPP
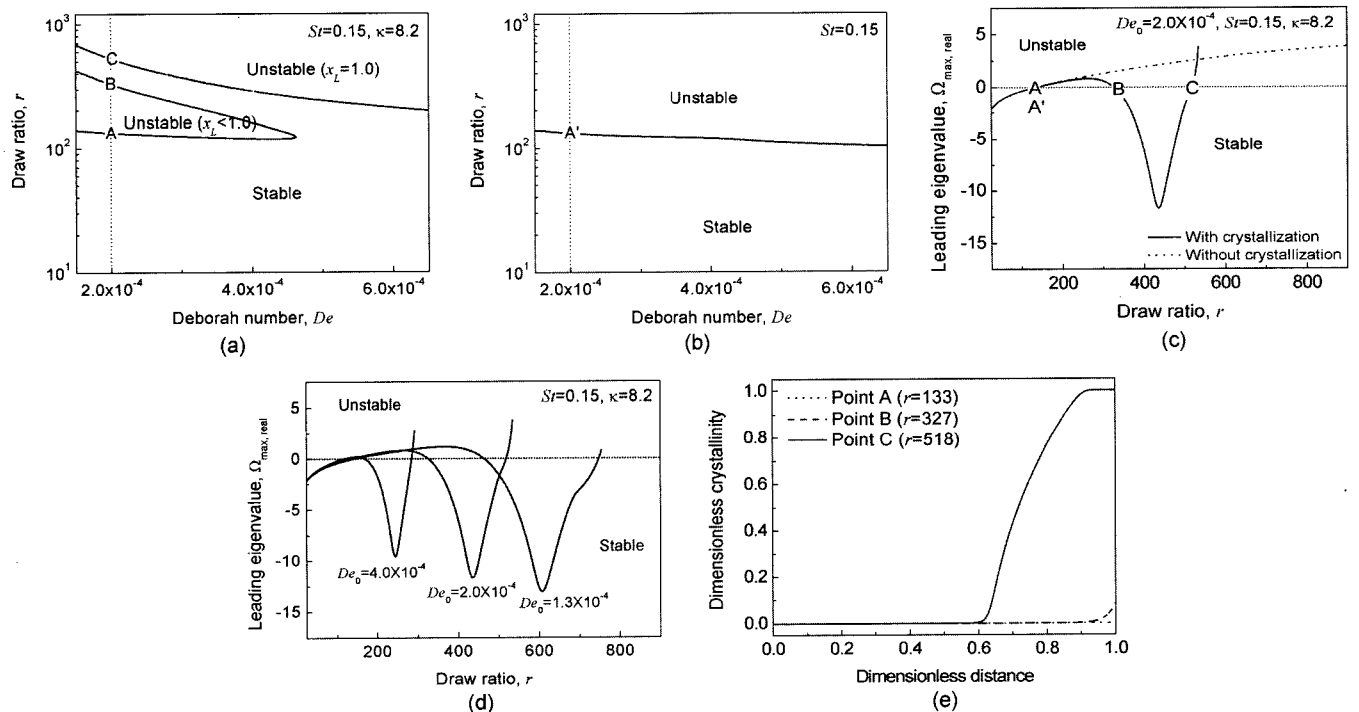

Fig. 2. Stability windows of iPP spinning depending on the Deborah number at $St = 0.15$ (a) with and (b) without crystallization. Real part of leading eigenmode of the spinning process with respect to draw ratio for (c) crystallization and (d) fluid viscoelasticity, and (e) crystallization profiles pointed out on Fig. 2(c).

spinning model. Figs. 2a and 2b show the stability diagrams of the systems with and without crystallization, respectively, with the varying fluid viscoelasticity or Deborah number. The lower draw ratio bounds for the given Deborah numbers are almost the same in both cases, because the effect of FIC on the spinline is insignificant under these conditions. Interestingly, the spinning process with crystallization involves the second stable region with high draw ratio values shown in Fig. 2a, not found in the case with no crystallization in Fig. 2b, as will be explained below.

These neutral stability curves have been obtained looking at the real part of the leading eigenvalue as shown in Fig. 2c where the real parts of the leading eigenvalues are plotted against the draw ratio under the given process conditions. For example, three onset points, A, B, and C at the fixed Deborah number $(De = 2.0 \times 10^{-4})$ in Fig. 2a are found from Fig. 2c when the real part of the eignevalues becomes zero, i.e., meaning the onset points of the stability. There is only one crossing point in Fig. 2c for the no-crystallization case, A', and thus there is only one curve in Fig. 2b. (The points of A and A' are very close to each other because the crystallization effect at smaller draw ratios is minimal).

Fig. 2d shows different Deborah number cases revealing the destabilizing effect of the increasing Deborah number at upper draw ratio bound, i.e., iPP-like materials with $\xi = 0.6$ in the model. Fig. 2e shows different spinline crystallinity profiles at various onset points with different draw ratios, clearly showing whether the maximum crystallinity value is reached on the spinline at each case.

Figs. 3a and 3b display the stability windows of both cases with and without crystallization under a higher cooling condition, respectively, than that of Fig. 2. The stabilizing effect of the spinline cooling (Jung et al., 1999) in both cases is clearly seen comparing Figs. 2a and 3a, and Figs. 2b and 3b, respectively. It is interesting to notice that in the crystallization case of Figs. 3a and 3c, high cooling condition makes the middle unstable region shown in Fig. 2a disappear, and also this prompts the fully developed crystallinity on the spinline, which has the destabilizing effect, leading to lower draw ratio onsets than the corresponding curve in Fig. 2a.

The effect of spinline cooling (Stanton number in this study) on the process stability with and without crystallization is further displayed in Fig. 4a and 4b, respectively. The upper unstable region in the crystallization case in Fig. 4a caused by the maximum crystallinity reached on the spinline does not exist in Fig. 4b when there is no crystallization and cooling is large, i.e., a large St number.

The above linear stability analysis for the effect of flow-induced crystallization on spinning stability can make possible further stabilization and optimization strategies to enhance the productivity/profitability of the spinning pro-
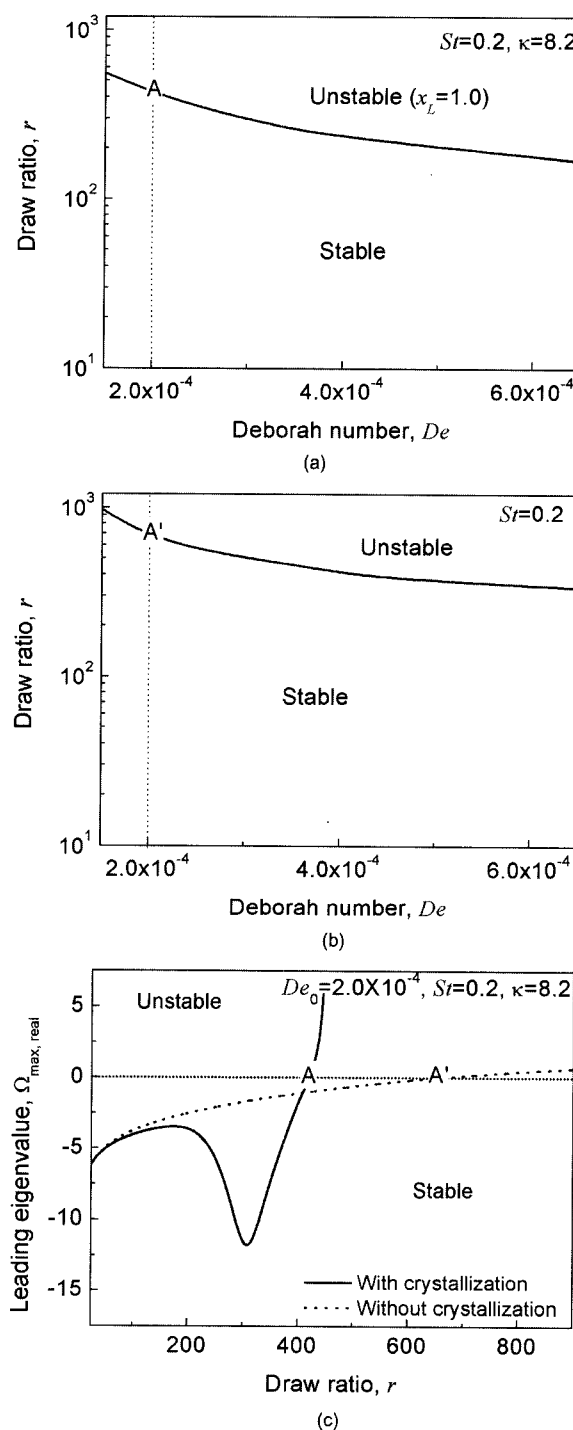

(a)

(b)

(c)

Fig. 3. Stability windows of iPP spinning depending on the Deborah number at $St = 0.2$ (a) with and (b) without crystallization, and (c) real part eigenvalue profiles with and without crystallization.

cess. The same approach should also be equally applicable to more complex spinning system, i.e., high-speed spinning with necking phenomena (Takaraka et al., 2004; Shin et al., 2005), and other extension deformation processes like
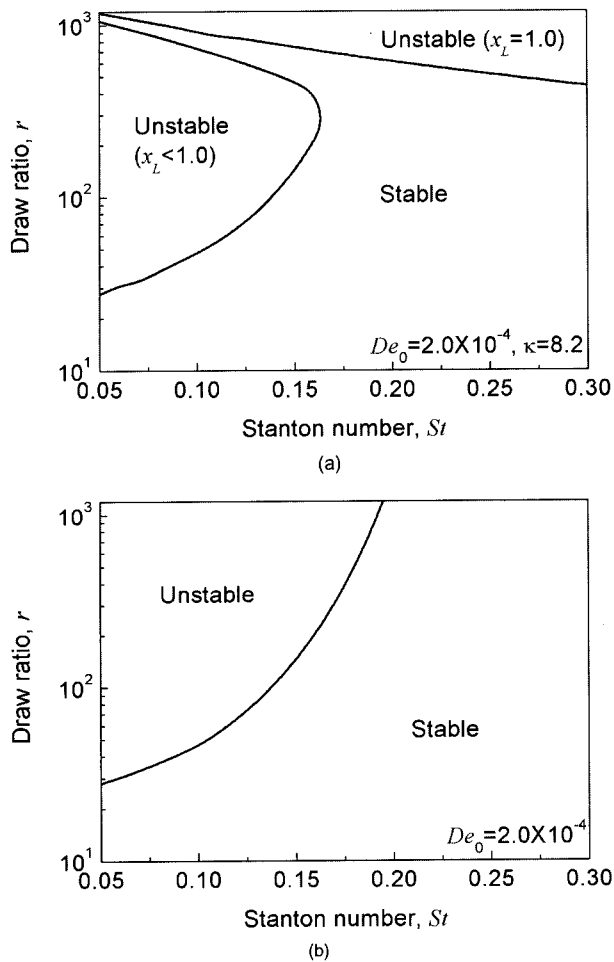
Fig. 4. Neutral stability curves of iPP spinning depending on the Stanton number or cooling (a) with and (b) without crystallization.

film casting and film blowing processes.

5. Conclusions

As a sequel to the paper by Lee et al. (2005b) which first reported the transient solutions of low-speed spinning with flow-induced crystallization, this study has further investigated the relationship between the crystallization kinetics and the various stability conditions of the iPP spinning using the linear stability method. It has been found that the flow-induced crystallization can give the stabilizing or destabilizing effect, depending on the extent of the spinline crystallinity. The crystallization generally stabilizes the spinning system when the crystallinity is not fully developed on the spinline, whereas it makes the system more unstable or less stable when it is fully developed to its maximum value. It is believed that the destabilizing effect of the FIC in low-speed spinning with maximum crystallinity on the spinline is due to the reduction of the real spinning distance available for deformation on the spinline.

These linear stability results agree with those by nonlinear transient simulation, as first conducted by Lee et al. (2005b).

References

Christensen, R.E., 1962, Extrusion coating of polypropylene, S. P. E. J. **18**, 751.

Doufas, A.K., A.J. McHugh and C. Miller, 2000a, Simulation of melt spinning including flow-induced crystallization. Part I. Model development and predictions, J. Non-Newtonian Fluid Mech. **92**, 27.

Doufas, A.K., A.J. McHugh, C. Miller and A. Immaneni, 2000b, Simulation of melt spinning including flow-induced crystallization. Part II. Quantitative comparisons with industrial spinline data, J. Non-Newtonian Fluid Mech. **92**, 81.

Fisher, R.J. and M.M. Denn, 1976, A theory of isothermal melt spinning and draw resonance, AIChE J. **22**, 236.

Gelder, D., 1971, The stability of fiber drawing processes, Ind. Eng. Chem. Fundam. **10**, 534.

Hatzikiriakos, S.G. and K. Migler (ed.), 2005, Polymer processing instabilities: Control and understanding, Marcel Dekker, New York.

Hyun, J.C., 1978, Theory of draw resonance: I. Newtonian fluids, AIChE J. **24**, 418, also, Part II. Power-law and Maxwell fluids **24**, 423.

Joo, Y.L., J. Sun, M.D. Smith, R.C. Armstrong, R.A. Brown and R.A. Ross, 2002, Two-dimensional numerical analysis of non-isothermal melt spinning with and without phase transition, J. Non-Newtonian Fluid Mech. **102**, 37.

Jung, H.W., H.-S. Song and J.C. Hyun, 1999, Analysis of the stabilizing effect of spinline cooling in melt spinning, J. Non-Newtonian Fluid Mech. **87**, 165.

Jung, H.W., H.-S. Song and J.C. Hyun, 2000, Draw resonance and kinematic waves in viscoelastic isothermal spinning, AIChE J. **46**, 2106.

Kolb, R., S. Seifert, N. Stribeck and H.G. Zachmann, 2000, Simultaneous measurements of small- and wide-angle X-ray scattering during low speed spinning of poly(propylene) using synchrotron radiation, Polymer **41**, 1497.

Lee, J.S., H.W. Jung, J.C. Hyun and L.E. Scriven, 2005a, A simple indicator of draw resonance instability in melt spinning processes, AIChE J. In print.

Lee, J.S., D.M. Shin, H.W. Jung and J.C. Hyun, 2005b, Transient solutions of the dynamics in low-speed fiber spinning process accompanied by flow-induced crystallization, J. Non-Newtonian Fluid Mech. Being reviewed.

Liu, B and A.N. Beris, 1988, Time-dependent fiber spinning equations. 2. Analysis of the stability of numerical approx-

imation, *J. Non-Newtonian Fluid Mech.* **26**, 363.

Matsumoto and Bogue, 1978, Draw resonance involving rheological transitions, *Polym. Eng. Sci.* **18**, 564.

Miller, J.C., 1963, Swelling behavior in extrusion, *S. P. E. Trans.* **3**, 134.

Minoshima, W., J.L. White and J.E. Spruiell, 1980, Experimental investigation of the influence of molecular weight distribution on the rheological properties of PP melts, *Polym. Eng. Sci.* **20**, 1166.

Muslet, I.A. and M.R. Kamal, 2004, Computer simulation of the film blowing process incorporating crystallization and viscoelasticity, *J. Rheol.* **48**, 525.

Patel, R.M., J.H. Bheda and J.E. Spruiell, 1991, Dynamics and structure development during high-speed melt spinning of nylon 66. II. Mathematical modeling, *J. Appl. Polym. Sci.* **42**, 1671.

Petrie, C.J.S., 1988, Some remarks on the stability of extensional

flows. *Progress and Trends in Rheology* **II**, 9.

Phan-Thien, N., 1978, A nonlinear network viscoelastic model, *J. Rheol.* **22**, 259.

Schultz, W.W., A. Zebib, S.H. Davis and Y. Lee, 1984, Nonlinear stability of Newtonian fibres, *J. Fluid Mech.* **149**, 455.

Shin, D.M., J.S. Lee, H.W. Jung and J.C. Hyun, 2005, Dynamics and stability of high-speed spinning process accompanied by flow-induced crystallization, Submitted to Rheol. Acta.

Takarada, W., K. Kazama, H. Ito and T. Kikutani, 2004, High-speed melt spinning of polypropylene terephthalate with periodic oscillation of take-up velocity, *Intern. Polym. Proc.* **XIX**, 4.

Zheng, R. and P. K. Kennedy, 2004, A model for post-flow induced crystallization: General equations and predictions, *J. Rheol.* **48**, 823.

Ziabicki, A., 1976, *Fundamentals of fiber formation*, Wiley-Interscience, New York.